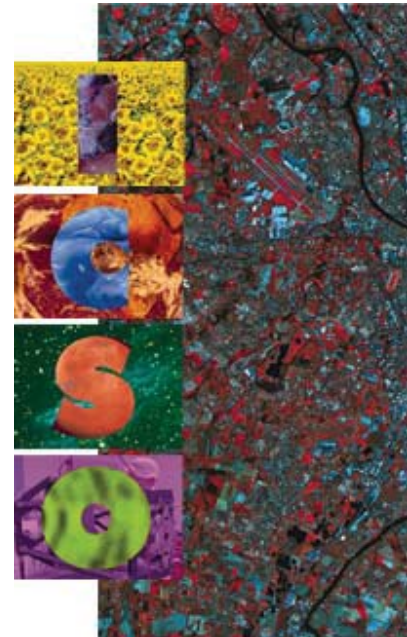


# International Conference on Space Optics—ICSO 2000

Toulouse Labège, France

5–7 December 2000

*Edited by George Otrio*



## *Active optics and corrective holographic gratings: a general recording method applied to COS/HST 2003*

*Gerard R. Lemaitre, Michel Duban*



## Active optics and corrective holographic gratings

### A general recording method applied to COS / HST 2003

G rard R. Lema tre<sup>a</sup> & Michel Duban<sup>b</sup>

Observatoire Astronomique de Marseille Provence

(<sup>a</sup>) 2 Place Le Verrier, 13248 Marseille CX4, France

(<sup>b</sup>) 1 All e Peiresc, 13376 Marseille CX12, France

#### 1. Multimode Deformable Mirrors

*Aberration corrected gratings* are useful to design spectrographs having the minimum of optical surfaces, thus minimizing light loss such as needed for astronomical instruments. For instance, many space orbiter spectrographs for the uv and euv are using as sole optics a single concave grating. Basically, the holographic recording process requires the formation of an interference pattern which is frozen into the photosensitive layer of the grating substrate. One of the two recording wavefronts must be aspheric in order to obtain aberration corrections. Up to now, the formation of an aspheric wavefront requires to design and built a special optical system providing the opposite shape of the wavefront to be corrected. Generally, such a compensating system is complex, expensive and only usable for making a particular grating. Also, various type of aberrations cannot be simultaneously achieved with such optical systems, therefore leading to great difficulties for correcting high order aberrations with holographic gratings.

A general method for recording corrected diffraction gratings without requiring to the above sophisticated optical systems, has been conceived (Duban & Lema tre 1998). This uses a plane *multimode deformable mirror* (MDM) (Lema tre & Wang 1995). The MDM provides a quasi-all-order optical path compensator which should give rise to a **universal recording method**.

As an exemple of the method, one have considered the recording of the three holographic gratings of the HST Cosmic Origins Spectrograph (COS) (Green 1998, Morse *et al.* 1998). Very substantial improvements in the image quality has been found (Duban 1998, Lema tre & Duban 1998) by use of a MDM as *recording compensator*. The result is that i) much higher order aberrations can simultaneously be corrected, and therefore ii) the residual blur images of the spectra occupy  $\simeq 25$ -30 times smaller areas than those obtained up to now. Thus, this new method provides large 2D gains i.e. both in spectral resolution and in limiting magnitude.

The elasticity design, object of the present analysis, has been investigated at the Laboratoire d'Optique de l'Observatoire de Marseille (LOOM) and has been followed up by the construction and performance evaluation of active *vase form* mirrors fitted with radial arms. This concept provide the basic features of *multimode deformable mirrors*. Drum form mirrors have been suggested in the past by Couder (1931) for making lighten mirrors. Vase form mirrors are quite similar to those mirrors. With the first 12-arm MDM design and optical evaluation (Lema tre & Wang 1995 and Moretto & Lema tre 1995), the analysis shows the strong mathematical link between the elasticity theory i.e. *Clebsch's polynomials* and the optical theory of aberrations i.e. the wavefront polynomials or *Zernike's polynomials*. We propose to name this active optics modes *Clebsch-Zernike polynomials*.

*Active optics methods*, pioneered by B. Schmidt, already lead to high performance concepts for large telescopes (ESO NTT and VLT primaries, CFHT, THEMIS and TEMOS 4 secondaries, Keck primary segments, LAMOST primary and secondary segments), for astronomical interferometry in the visible (highly variable curvature mirrors for the delay lines of the VLTI), as well as for focal instrumentation (axisymmetric and non-axisymmetric aspherized mirrors and gratings).

## 2. Elasticity design of a vase form MDM in the CTD class

Active MDM compensators for new grating recording methods have to realize the coaddition of many deformation modes such as, for instance, a 1st order curvature mode  $Cv\ 1$ , 3rd order modes  $Sphe\ 3$ ,  $Coma\ 3$ ,  $Astm\ 3$ , and 5th order modes  $Astm\ 5$ , and  $Tri\ 5$ , the latter mode being of tertiary symmetry. This contracted denotation is useful and usual in opticians' terminology. If needed, higher order modes could be compensated by an adaptive system. However, the elasticity theory shows that higher order modes could also be generated.

Given the number of modes to be generated and the difficulty of easily superposing more than two modes with mirrors belonging to the Variable thickness distribution (VTD) class (Lemaître 1989), a mirror belonging to the Constant thickness distribution (CTD) class has been investigated. A preliminary goal was to match up the number of actuators with the geometrical modes to achieve. It has been found that forces applied onto discrete azimuths equally distributed along the mirror perimeter would be optimal for generating axi and non-axisymmetry modes. An important aspect of the design is the fact that the discrete position actuators have to generate, in both radial and tangential directions, a smooth and continuous deformation at the proximity of the boundaries. The shear component of the deformation due the punctual forces provide a slope discontinuity at position where the force apply. This component has a much more local effect and is of much smaller amplitude that the bending component of the deformation, but nevertheless it is preferable to minimize the shear component by avoiding pontual forces directly applied onto the optical surface even at the mirror edge. For continuity reasons, these pontual forces has to be applied at some distance from the optical surface such us presented here.

Following the Saint-Venant's principle (see Germain & Muller 1994) led to the design of a *vase form*, i.e. a mirror having two concentric zones of *constant rigidity* (Lemaître 1980). The outer zone is thicker than that of the clear aperture which is the inner zone. The two zones are clamped together and ponctual forces are applied onto the outer ring. Apart from minimizing the shear deformation to a negligible value at the optical surface, another advantage a thicker ring is to provide a *regular modulation of the tangential deformation* generated by discrete forces. Because of large axial forces and important tangential moments to apply on the outer ring, several radial arms have been found preferable to complete the mirror design.

Fig.1 - Elasticity design of a *multimode deformable mirror* - MDM - showing a *two-zone* rigidity and radial arms. The clear aperture zone is built-in at  $r=a$  into a thicker ring. The *holosteric* shape allows one to achieve the Clebsch-Zernike deformation modes i.e.  $Cv\ 1$ ,  $Sphe\ 3$ ,  $Coma\ 3$ ,  $Astm\ 3$ ,  $Astm\ 5$ ,  $Tri\ 5$ ,  $Tri\ 7$ ,  $Squa\ 7$ ,  $Squa\ 9$ , ... by the action of axial forces  $F_{a,k}$  and  $F_{c,k}$  applied to the ring inner radius  $r=a$  and to the outer end  $r=c$  of each arm (here  $k_m=12$  arms). Except for the mode  $Sphe\ 3$  which is achieved by addition of uniform air pressure or depressure  $q$ , all other above modes, obtained with  $q=0$ , belong to the central and upper-adjacent diagonals of the optics triangular matrix.

Figure 1 displays the basic design of a *multimode deformable mirror*. The clear aperture zone  $0 < r < a$ , is built-in into a thicker outer ring  $a < r < b$ , so that the mirror can be easily machined as a *holosteric* piece. Both axial forces and tangential torques will be applied to the discrete positions of the outer ring. Each actuator is able to generate a positive or a negative axial force. The forces applied at the internal circle  $r = a$  are denoted  $F_{a,k}$ ; those applied at the external circle  $r = c$  are denoted  $F_{c,k}$  with here  $k_m=12$  arms i.e.  $k \in [1,2,...12]$ . In addition, positive or negative uniform loads  $q$  can be superposed into the vase inner zone by mean of air pressure or depressure.

Let us consider a plane MDM and denote  $E$  and  $\nu$  the Young's modulus and the Poisson's ratio respec-

tively,  $t_1, t_2$  and  $D_1, D_2$  the thicknesses and associated rigidities for inner and outer zones respectively. In cylindrical coordinates, the deflected surface  $Z$  is given by the Poisson's equation (Timoshenko & Woinowsky-Krieger 1959)

$$\nabla^2 \nabla^2 Z(r, \theta) = q/D \quad \text{with} \quad D = Et^3/[12(1-\nu^2)] = \text{constant}, \quad (1,2)$$

and  $\nabla^2 = \partial^2/\partial r^2 + \partial./r\partial r + \partial^2./r^2\partial\theta^2$  the laplacian,  $D=D_1$  for  $0 < r < a$ ,  $D=D_2$  for  $a < r < b$ .

- On the inner zone of the vase mirror, a polynomial representation of the deformation in cylindrical coordinates is expressed as

$$Z = \sum z_{nm} = \sum A_{nm} r^n \cos m\theta, \quad (3)$$

where  $n$  and  $m$  are positive integers,  $(n+m)$  is *even* and  $A_{nm}$  coefficients belong to the triangular matrix expressing the optical path differences, i.e.  $m \leq n$ . For a given mode  $z_{nm}$ , substitution in Eq.(1) leads to

$$A_{nm}(n^2 - m^2)[(n-2)^2 - m^2]r^{n-4} \cos m\theta = q/D \quad \text{with} \quad n \geq 2. \quad (4)$$

– For  $q = 0$  in Eq.(1), one finds two classes of solutions,  $m = n$  i.e.  $A_{22}, A_{33}, A_{44}, \dots$  terms and  $m = n - 2$  i.e.  $A_{20}, A_{31}, A_{42}, A_{53}, \dots$  terms.

– For  $q = \text{constant}$ , one finds  $n = 4$  simultaneously with  $m = 0$  i.e. the  $A_{40}$  term.

This shows that the generation of  $A_{20} - Cv1$ ,  $A_{40} - Sphe3$ ,  $A_{31} - Coma3$ ,  $A_{22} - Astm3$ ,  $A_{42} - Astm5$ ,  $A_{33} - Tri5$ ,  $A_{53} - Tri7$ ,  $A_{44} - Squa7$ , ... modes is obtained, while it is found not possible to generate the  $A_{51} - Coma5$  or  $A_{60} - Sphe5$  modes by using a uniform loading  $q = \text{constant}$ . A parabolic loading would be required in this case so that  $A_{40}, A_{60}$  and  $A_{51}$  could not be simultaneously set at any given values.

- On the outer zone of the vase mirror, a uniform load is never applied, so that the equation to be solved for  $a < r < b$  is Eq.(1) with  $q = 0$ . The solutions are

$$Z = \sum z_{nm} = R_{n0} + \sum_{m=1}^{\infty} R_{nm} \cos m\theta + \sum_{m=1}^{\infty} R'_{nm} \sin m\theta, \quad (5)$$

in which  $R_{n0}, R_{n1}, \dots, R'_{n1}, \dots$  are function of the radial distance only. In our case, one considers the same azimuth of the deformation as that given by Eq.(4), so that the third functions  $R'_{nm}$  vanish. The functions  $R_{nm}$  are Clebsch's solutions of

$$\left(\frac{d^2}{dr^2} + \frac{1}{r} \frac{d}{dr} - \frac{m^2}{r^2}\right) \left(\frac{d^2 R_{nm}}{dr^2} + \frac{1}{r} \frac{dR_{nm}}{dr} - \frac{m^2}{r^2} R_{nm}\right) = 0. \quad (6)$$

For  $m = 0, m = 1$  and  $m > 1$ , the functions  $R_{nm}$  have the following forms

$$\begin{aligned} R_{n0} &= B_{n0} + C_{n0} \ln r + D_{n0} r^2 + E_{n0} r^2 \ln r, \\ R_{n1} &= B_{n1} r + C_{n1} r^{-1} + D_{n1} r^3 + E_{n1} r \ln r, \\ R_{nm} &= B_{nm} r^m + C_{nm} r^{-m} + D_{nm} r^{m+2} + E_{nm} r^{m+2}. \end{aligned} \quad (7)$$

The boundaries between the two zones at  $r = a$  must provide a continuity of the flexure  $z_{nm}$ , slope  $dz_{nm}/dr$ , bending moment  $M_r$  and shearing force  $Q_r$

$$M_r = -D \left[ \frac{\partial^2 z}{\partial r^2} + \nu \left( \frac{1}{r} \frac{\partial z}{\partial r} + \frac{1}{r^2} \frac{\partial^2 z}{\partial \theta^2} \right) \right], \quad Q_r = -D \frac{\partial}{\partial r} (\nabla^2 z). \quad (8)$$

Denoting  $\gamma = D_1/D_2$  as the *rigidity ratio* between the two zones ( $\gamma < 1$ ), for  $\forall\theta$ , the four continuity conditions provide the coefficients  $B_{nm}, C_{nm}, D_{nm}$  and  $E_{nm}$  in Eqs.7 by respect to  $A_{nm}$  and allow the determining the distributions of bending moments  $M_r(r, \theta)$  and shearing forces  $Q_r(r, \theta)$ , applied to the ring and namely at its edge  $r = b$ . These determinations are done for each considered mode.

For example, one finds for the 5th order astigmatism mode, i.e.  $n = 4, m = 2, A_{42} - Astm5$

$$\begin{aligned} B_{42} &= 3(1 - \gamma)a^2 A_{42}/2, \\ C_{42} &= -(1 - \gamma)a^6 A_{42}/2, \\ D_{42} &= \gamma A_{42}, \\ E_{42} &= 0, \\ M_r(b) &= -2D_2[(1 - \nu)B_{42} + 3(1 - \nu)C_{42}/b^4 + 6D_{42}b^2 - 2\nu E_{42}/b^2], \\ Q_r(b) &= -8D_2[3D_{42}b + E_{42}/b^3]. \end{aligned}$$

In order to realize  $M_r$  and  $Q_r$  at  $r=b$ , it is to be noticed that the MDM design gains in *compactness* by applying the axial forces at  $r=a$  and  $r=c$  instead of at  $r=b$  and  $r=c$ . With this choice, the axial forces are denoted  $F_{a,k}$  and  $F_{c,k}$  (cf. Fig. 1) and defined by the statics equilibrium relationships

$$F_{a,k} + F_{c,k} = b \int_{\pi(2k-3)/k_m}^{\pi(2k-1)/k_m} Q_r(b, \theta) d\theta, \quad (9 - a)$$

$$(b - a)F_{a,k} + (b - c)F_{c,k} = b \int_{\pi(2k-3)/k_m}^{\pi(2k-1)/k_m} M_r(b, \theta) d\theta, \quad (9 - b)$$

with  $k = 1, 2, \dots, k_m$  for a MDM having  $k_m$  arms.

The  $F_{a,k}$  and  $F_{c,k}$  are determined for each mode  $A_{nm}$  by starting from the corresponding equation set  $B, C, D, E$  provided by the continuity conditions and then allowing to express  $M_r(b), Q_r(b)$ .

### 3. A 6-arm MDM elasticity design for a Clebsch-Zernike 6-mode coaddition

A 6-arm multimode deformable mirror has been designed which is able to provide the coaddition of 6 Clebsch-Zernike modes. This is for developping the new recording method of holographic gratings and particularly to the case of the Cosmic Origins Spectrograph of HST 2002.

Compared to glass or vitrocera materials, metal mirrors present several features that are of interest in the achievement of large deformaton active surfaces. The gain in *flexibility-ratio*  $\sigma_{lim}/E$ , is larger than 100. This is basically due to the much higher yield strength  $\sigma_{lim}$  of metal alloys. Two other selective criteria for selecting metal substrates are a perfect *stress-strain linearity* in the sense of Hooke's law and a *broad elastical range*. With respect to these criteria, quenched FeCr13 is well know, otherwise metal alloys such CuNi18Zn20 or TiAl6V4 could be experimented, but Al predominant alloys show more restrictive linear ranges and are impossible to polish without metal overcoat.

A performance evaluation has been carried out with two prototype MDMs. Their optical figure were flat while at rest and having a clear aperture of 8 cm. The selected metal alloy was FeCr13, since this is a material that has a long term experience at LOOM. After this selection, the optimization of a convenient flexibility has been done by determining the rigidities  $D_1$  and  $D_2$  i.e. the thicknesses  $t_1$  and  $t_2$ , with respect to the maximum stress. The maximum stress has been kept lower than the yield strength of the FeCr13 material which is 1200 N/mm<sup>2</sup>. This does not take into account a possible *quenching* process of this material that could substantially increases this limit if necessary in a further stage. In order to respect the 3D homogeneity of the substrate, the 6 radial arms were not added to the vase mirror but machined into the substrate in a one piece device by a numerical command machine. The deformations are obtained by control of the rotation of 9 differential screws linked between the arms and the support; the 3 remaining screws located at  $\theta = 0, \pm 2\pi/3$  and  $r = a$  are not active since defining the reference plane of the deformations. The geometrical parameters of the 6-arm MDM are displayed by Figure 2.

Fig.2 - True proportion design of the 6-arm MDMs in quenched FeCr13 alloy. The elastic constants are  $E=2.05 \times 10^4$  daN.mm $^{-2}$  and  $\nu=0.305$  for the Young's modulus and the Poisson's ratio respectively. The mirror geometry is defined by the thicknesses  $t_1=5$  mm and  $t_2=14$  mm for the central plate and outer ring respectively. The radial parameters are  $a=40$  mm,  $b=54$  mm and  $c=80$  mm. This geometry provides a rigidity-ratio  $1/\gamma = D_2/D_1 = (14/5)^3 \simeq 22$  and an aspect ratio  $2a/t_1 = 16$ . The axial forces  $F_{a,k}$  and  $F_{c,k}$  are applied to the ring inner radius  $r=a$  and to the outer end  $r=c$  of the radial arms ( $k_m=6$ ) built-in to the ring.

The axial distribution of forces  $F_{a,k}$  and  $F_{c,k}$  applied to the MDM has been determined for each of 6 Clebsch-Zernike modes having a PtV deformation of  $1 \mu\text{m}$  at  $r=a=40$  mm for  $\theta \in [0, 2\pi]$ . This result is displayed by Table 1.

TABLE 1 - Axial distribution of forces  $F_{a,k}$  and  $F_{c,k}$  applied to a 6-arm MDM. The amplitude of the modes  $z_{nm} = A_{nm} r^n \cos m\theta$  has been set for a PtV deformation of  $1 \mu\text{m}$  at  $r=a=40$  mm for  $\theta \in [0, 2\pi]$ , thus corresponding to  $A_{20} = 6.250\text{E-}7$ ,  $A_{40} = 3.90625\text{E-}10$ ,  $A_{22} = A_{20}/2$ ,  $A_{31} = 7.8125\text{E-}9$ ,  $A_{33} = A_{31}$  and  $A_{42} = A_{40}/2$ . in  $\text{mm}^{1-n}$

		<i>Cv1</i>		<i>Sph3*</i>		<i>Astm3</i>		<i>Coma3</i>		<i>Tri5</i>		<i>Astm5</i>	
$\theta$		$n = 2, m = 0$		$n = 4, m = 0$		$n = 2, m = 2$		$n = 3, m = 1$		$n = 3, m = 3$		$n = 4, m = 2$	
$k$		$F_{a,k}$	$F_{c,k}$										
0	1	-2.327	2.327	-11.088	6.157	1.666	0.698	-3.271	1.823	8.792	4.415	-6.319	3.532
$\pi/3$	2	-2.327	2.327	-11.088	6.157	-0.833	-0.349	-1.635	0.911	-8.792	-4.414	3.160	-1.766
$2\pi/3$	3	-2.327	2.327	-11.088	6.517	-0.833	-0.349	1.635	-0.911	8.792	4.415	3.160	-1.766
$\pi$	4	-2.327	2.327	-11.088	6.157	1.666	0.698	3.271	-1.823	-8.792	-4.415	-6.319	3.532
$4\pi/3$	5	-2.327	2.327	-11.088	6.157	-0.833	-0.349	1.635	-0.911	8.792	4.415	3.160	-1.766
$5\pi/3$	6	-2.327	2.327	-11.088	6.157	-0.833	-0.349	-1.635	0.911	-8.792	-4.415	3.160	-1.766

\* The required uniform loading for producing the *Sph3* mode is  $q=0.005886$  daN.mm $^{-2}$

#### 4. Optical design of the COS gratings and MDM, recording parameters

The three COS gratings must correct the residual spherical aberration of the Hubble Space Telescope (HST). Therefore it is not possible to keep the grating substrates purely spherical. Thus we have introduced fourth and sixth degree deformations on the grating substrates, i.e.  $z_{40}$  and  $z_{60}$  terms.

Since the COS incident beam is located 5.40 arcmin off the HST optical axis, we also have been led to correct the HST astigmatism which produces an astigmatism length of 1.20 mm. The three holographic gratings use the Optimized Rowland Mounting (Duban 1987, Duban 1991) in such a way that the recording parameters cancel the astigmatism at two points  $P1$  and  $P2$  of the spectrum. We have demonstrated that, as a very general result which is also valid for the COS gratings, this mounting is the only one really suitable for obtaining the *Astm3* compensation.

Table 2 displays the spectral data in  $\text{\AA}$  and Table 3 displays the grating parameters, where  $N$  is the groove density in  $l.\text{mm}^{-1}$ ,  $R$  the radius of curvature of the grating substrates in mm,  $\lambda_0$  the laser recording wavelength,  $i$  the incidence angle at the HST,  $\alpha$  and  $\beta$  the recording angles in deg. Table 4 displays the deformation coefficients of the grating substrates in  $\text{mm}^{-n+1}$ . Substrates of gratings #1 and #2 are identical. Table 5 displays the deformation coefficients in  $\text{mm}^{-n+1}$  and the incidence angle  $i_{\text{MDM}}$  upon the MDM in deg. For the recording, the distance from the laser source 1 to the MDM is 1100 mm for gratings #1 and #2, and 1000 mm for grating #3. Of course, all the parameters can easily be modified slightly, if necessary, in order to exactly match the COS geometry of detector positioning.

TABLE 2. Spectral data in Å

Grating	$\lambda_{\min}$	$P1$	$\lambda_{\text{med}}$	$P2$	$\lambda_{\max}$
#1	1150	1185	1295.5	1382	1449
#2	1405	1456	1589.5	1684	1774
#3	1230	1320	1615.0	1810	2000

TABLE 3. Grating and geometrical recording parameters

Grating	$N$	$R$	$\lambda_0$	$i$	$\alpha$	$\beta$
#1	3800	1652.0	3511	19.886	-36.089	48.171
#2	3052.6	1652.0	3511	19.538	-25.750	39.592
#3	380	1613.4	4880	2.106	-4.025	6.618

TABLE 4. Substrate coefficients  
[deformation sags in  $\mu\text{m}$ ]

Grating	$A_{40}$	$A_{60}$
#1	1.913E-9	9.14E-14
	[2.68]	[0.15]
#2	1.913E-9	9.14E-14
	[2.68]	[0.15]
#3	1.822E-9	1.03E-13
	[2.33]	[0.15]

TABLE 5. MDM coefficients and incidence angle

Grating	$A_{31}$	$A_{33}$	$A_{42}$	$i_{\text{MDM}}$
#1	4.821E-8	-5.582E-8	-2.172E-9	29.96°
#2	1.880E-8	-2.671E-8	-2.360E-9	16.92°
#3	0.512E-8	-0.003E-8	-0.180E-9	10.00°

Spot diagrams are calculated at five wavelengths for each grating as displayed in Figs. 3, 4 and 5. The wavelengths in Å are those listed in Table 2 and correspond - from left to right - to  $\lambda_{\min}$ ,  $P1$ , the middle of the spectrum  $\lambda_{\text{med}}$ ,  $P2$ , and  $\lambda_{\max}$ . The correction of astigmatism at points  $P1$  and  $P2$  is evident. The resolving power of the  $f/24$  HST images at the input of COS is  $1.22 \lambda f/d = 3.8 \mu\text{m}$  at  $1300 \text{Å}$  and the concave gratings provide a magnification  $\simeq -1$ . Despite of the simplification here provided by axisymmetric

Fig. 3 - Spot-diagram given by grating #1,  $3800 \text{ l.mm}^{-1}$ . Fig. 4 - Spot-diagram given by grating #2,  $3052.6 \text{ l.mm}^{-1}$ .Fig. 5 - Spot-diagram given by grating #3,  $380 \text{ l.mm}^{-1}$ .

grating substrates, the images given by gratings #1 and #2 are diffraction limited with respect to the resolution over the main part of the spectral range, and are very nearly diffraction limited at the extremities. In addition, the image heights have a similar size compared to our precedent studies. With

grating #3, of low dispersion, both the widths and the heights of the images remain diffraction limited. In Figs. 2, 3 and 4 and for each color,  $\Delta$  is the focusing onto the principal ray with respect to the Rowland circle. A positive  $\Delta$  means an increase of the image distance to the grating vertex. The geometrical scheme of the recording mounting is displayed by Fig. 6. This mounting is easier to practice than conventional ones.

Fig.6 - Basical recording mounting. The recording angles  $\alpha$  and  $\beta$  i.e. principal rays at the vertex  $O$  of the grating from laser source points  $L_1$  and  $L_2$  respectively are given by Table 3. For the case of COS grating #1, the incidence angle at the vertex  $M$  of the MDM is  $i_{\text{MDM}}=29.96^\circ$ . The Rowland circle optical paths are  $L_1O = R \cos \alpha$  and  $L_2O = R \cos \beta$  with  $R=1652$  mm and  $L_1M=1100$  mm.

Compared to the FWHM size of blur images obtained by the COS team (Osterman *et al.* 2000) with pixel size of  $2.4 \times 33 \mu\text{m}^2$  and with grating #1 (3800 l/mm), our design provides very effective 2D gains in resolution and sensitivity :

- 1) for all three gratings, the COS spectral resolution  $\lambda/\delta\lambda$  would be increased by a factor 10,
- 2) in addition, for the two more dispersive gratings, the limiting magnitude (perpendicular direction) is higher, i.e. the COS sensitivity on the sky appears to be increased of  $\simeq 1-1.2$  mag.

## 5. The 6-arm MDM compensating a 3-mode coaddition for the COS gratings

The 6-arm MDM described in Section 3 has been built in two samples for a development recording of the COS holographic grating. With the previous optimizations, the grating substrates are axisymmetric aspherics - mainly due to the HST primary mirror shape - and the holographic recording requires the coaddition of three aberration modes  $A_{31}$ ,  $A_{33}$  and  $A_{42}$  such as given in Table 5. A 6-arm MDM is particularly convenient to achieve this coaddition. The axial forces  $F_{a,k}$  and  $F_{c,k}$  applied on each end of the clamped arms are given in Table 6.

TABLE 6. 6-arm MDM. Axial distribution of forces  $F_{a,k}$  and  $F_{c,k}$  for the recording of the COS grating #1 i.e. 3800 l/mm. The MDM geometrical parameters are the same as those given in Table 1. The amplitudes of the three coadded modes  $z_{nm} = A_{nm} r^n \cos m\theta$ , are  $A_{31} = 4.821 \text{ E-}8$ ,  $A_{33} = -5.582 \text{ E-}8$  and  $A_{42} = -2.172 \text{ E-}9$  in  $\text{mm}^{1-n}$ .

[Units: daN]									
Angle	Arm	Coma3		Tri5		Astm5		Coaddition*	
$\theta$	nb. $k$	$n = 3, m = 1$ $F_{a,k}$	$F_{c,k}$	$n = 3, m = 3$ $F_{a,k}$	$F_{c,k}$	$n = 4, m = 2$ $F_{a,k}$	$F_{c,k}$	$F_{a,k}$	$F_{c,k}$
0	1	-20.180	11.249	-62.798	-31.540	70.275	-39.276	-12.703	-59.567
$\pi/3$	2	-10.090	5.625	62.798	31.540	-35.138	19.638	17.570	56.803
$2\pi/3$	3	10.090	-5.625	-62.798	-31.540	-35.138	19.638	-87.845	-17.527
$\pi$	4	20.180	-11.249	62.798	31.540	70.275	-39.276	153.253	-18.985
$4\pi/3$	5	10.090	-5.625	-62.798	-31.540	-35.138	19.638	-87.845	-17.527
$5\pi/3$	6	-10.090	5.625	62.798	31.540	-35.138	19.638	17.570	56.803

(\*) These two columns display the resulting forces to be applied for obtaining the three mode coaddition. It can be noticed that the total resulting forces  $\mathcal{F}_a = \Sigma F_{a,k}$  and  $\mathcal{F}_c = \Sigma F_{c,k}$  obtained by summation over the full perimeters  $r = a$  and  $r = c$  respectively, are both equal to zero.

## 6. MDM tuning of the 3-mode coaddition for COS / HST

Figure 7 displays views of MDM #1 in its mounting and of the rear side of MDM #2 alone. Figure 8 displays single modes  $Cv\ 1$ ,  $Astm\ 3$ ,  $Coma\ 3$ ,  $Tri\ 5$  and  $Astm\ 5$  obtained with the 6-arm MDM #2. In accordance with Table 1, the mode  $Sphe\ 3$  could be obtained by applying some air pressure or depressure inside the MDM vase form. This equipment is not necessary for COS.

Fig.7 - Views of MDM #1 in its mounting - with the nine differential screws and three reference points onto the inner ring - and of MDM #2 alone.

Fig.8 - He-Ne interferograms of MDM #2 at full aperture 80mm showing single modes  $Cv\ 1$ ,  $Astm\ 3$ ,  $Coma\ 3$ ,  $Tri\ 5$  and  $Astm\ 5$ . By respect to Table 1,  $Sphe\ 3$  could be obtained by air pressure or depressure inside the MDM vase form.

From the data such as given by Table 5, a fringe map can be drawn in order to provide theoretical model of the deformation to achieve. For the case of the COS grating # 1, this reference map at  $\lambda_{HeNe}=632.8\text{ nm}$  is displayed by Figure 9. The  $F_{a,k}$  and  $F_{c,k}$  forces such as given by Table 6 have been generated to the MDM by use of a dynamometric wrench. The forces are applied to 9 differential screws that provide  $100\mu\text{m}$  displacement for a  $2\pi$  rotation. The 3 remaining points at  $r = a$  and  $\theta = 0, \pm 2\pi/3$  are not actuated but provide the reference plane of the deformation. In the case of COS grating #1, the obtained MDM shape at  $\lambda_{HeNe}$  is displayed by Figure 9.

Fig.9 - Full aperture He-Ne interferograms (80 mm) of MDM #1 tuned as optical path compensator for the holographic recording of the COS grating #1 (3800 l/mm). The three modes *Coma*3, *Tri*5 and *Astm*5 have been coadded by generating forces  $F_{a,k}$  and  $F_{c,k}$  such as given by Table 6. [*Up*] Obtained shape, [*Down*] Theoretical shape.

A 80 mm circular aperture of COS gratings - which is larger than the  $73.2 \times 68.8 \text{ mm}^2$  area lightened up by the f/24 HST incident beam for  $i=20^\circ$  - corresponds to a recording beam at the MDM of  $42.9 \times 53.3 \text{ mm}^2$  for gratings #1, and little smaller for #2 and #3. On this MDM recording area, the PtV deviation of the interferogram is better than  $0.2 \lambda_{\text{HeNe}}$ . This can be partly checked by the reader in making a convenient scaled up transparent from the synthetic interfereogram.

$y (\theta=0)$

## 7. Conclusion

Although the deflexure of a concave or convex MDM will not be exactly identical to the present case of plane MDMs, the analysis remains valid for curved optical surfaces up to  $f/4$  or  $f/3$ . The elasticity design is very similar to that of active Cassegrain mirrors in vitrocera glass already developed at LOOM, since using a *two-zone rigidity* design of the *vase* form. The outer ring provides the respect of Saint Venant's principle by avoiding slope discontinuities of the shear component that would be caused at the optical surface by punctual force applications. The linked arms provide the most accurate distribution of the tangential deformations with a minimum of actuators. In addition to the particular case for  $A_{40}$  which is not used for COS, the generation of *two families* deformation modes  $A_{nm}$  has been found. The first family of solutions is given by  $m=n$  i.e.  $A_{22}, A_{33}, \dots$  modes and the second by  $m=n-2$  i.e.  $A_{20}, A_{31}, \dots$  modes. We have named these active optics polynomials *Clebsch-Zernike modes*.

Plane and 6-arm MDMs designed as *aberration path compensators* provide easily the first six Clebsch-Zernike modes  $A_{20}, A_{40}, A_{31}, A_{22}, A_{42}$  and  $A_{33}$ . As presently shown and compared to the state of the art, our active optics method provides very effective 2D gains in resolution and sensitivity :

- for all three gratings, *the COS spectral resolution  $\lambda/\delta\lambda$  would be increased by a factor 10*, and
- in addition, for the two more dispersive gratings, the limiting magnitude (perpendicular direction) is higher, i.e. *the COS sensitivity on the sky appears to be increased of  $\simeq 1-1.2$  mag*.

Plane MDMs are useful for developing a new and **universal** method of producing high order corrected gratings by holographic recording. They will certainly bring a milestone to the constructing technology of holographic gratings. The MDM #1 has been cordially made available to the COS team and Jobin Yvon Corp. At the moment, COS is expected to be mounted on the HST in 2003.

## Acknowledgements

The authors are grateful towards R.F. Malina (OAMP and Berkeley), J.C. Green (Univ. Boulder), J. Flamand (Jobin-Yvon Corp.) who strongly have encouraged to do this development and to P. Joulé for the 3-D figures. The realization of 6-arm MDMs was supported by the Université de Provence and CNRS.

## References

- Clebsch A.R.F., 1862, in *Theorie der Elasticität fester Körper*, Teubner edit. Leipzig (French translation *Théorie de l'Elasticité des Corps Solides* with annotations and compléments by Saint-Venant and Flamant, Dunod edit.(1881))
- Couder A., 1931, Bulletin Astronomique, 2ème Série, Tome VII, Fasc. VI, Paris
- Cui Xiangqun, Yang Dehua, 1998, LAMOST, in *Advanced Technology Optical and IR Telescopes*, Proc. SPIE **3352**, 378-385
- Duban M., 1987, Holographic aspheric gratings printed with aberration waves, Appl. Opt., **26**, 4263-4273
- Duban M., 1991, Third-generation Rowland holographic mounting, Appl. Opt., **30**, 4019-4025
- Duban M., 1998, Theory of spherical holographic gratings recorded by use of a MDM, Appl. Opt., **37**, 7209-7213
- Duban M., 1999, Theory and computation of three Cosmic Origins Spectrograph aspheric gratings recorded with a MDM, Appl. Opt., **38**, 1096-1102
- Duban M., Lemaître G.R., Malina R., 1998, Appl. Opt., **37**, 16, 3438-3439
- Duban M., Dohlen K., Lemaître G.R., 1998, Appl. Opt., **37**, 31, 7214-7217
- Ferrari M. & Lemaître G.R., 1993, VCMs: Analysis of large deflection zoom mirrors, Astron. Astrophys., **274**, 12-18
- Ferrari M., 1994, Optique active et grandes déformations élastiques, Doctoral Thesis, Observatoire de Marseille,

- Germain P., Muller P., 1994, *Introduction à la mécanique des milieux continus*, Masson edit., Paris
- Green J.C., 1997, The Cosmic Origins Spectrograph / HST, in *Space Telescope and Instruments*, Kona, HI, Proc. SPIE **3346**, 265-270
- Kross J., 1997, *L'Oeil du Grand Tout*, Laffont edit., French translation of the 1987 Estonian work *Vastutuulelaev*, Ed. Kirjastus "Eesti Raamat". This is concerning the life of Bernhard Schmidt 1879-1935
- Lemaître G.R., 1976, Elasticity and vary-focal mirrors, *Comptes Rendus Acad. Sc.*, **282**, Serie B, 87-89
- Lemaître G.R., 1980, VASE FORM: Asphérisation par relaxation élastique, *Comptes Rendus Acad. Sc.*, **290**, B, 171-174
- Lemaître G.R., 1981, Active optics and elastic relaxation methods, in *Current Trends in Optics*, International Commission for Optics, Taylor & Francis eds., London, 135-149
- Lemaître G.R., 1983, Active reshaping of the CFHT Cassegrain mirror, Private communication to R. Racine, CFHT (see also CFHT Bulletin, P. Bely et al., 1984)
- Lemaître G.R. & Wang M., 1992, TÉMOS 4: Optical results with a segmented spherical primary and an actively aspherized secondary, in *Metal Mirrors*, University College of London, Proc. SPIE **1931**, 43-52
- Lemaître G.R., 1989, Various Aspects of Active Optics, in *Telescopes and Active Systems*, Orlando, FA, Proc. SPIE **1114**, 328-341
- Lemaître G.R., Duban M., 1998, MDMS: A general method of holographic grating recording, *Astron. Astrophys. Letter*, **339**, L89-L93
- Lemaître G.R. & Wang M., 1995, MDMS: Active mirrors warped using Zernike polynomials for correcting off-axis aberrations of fixed primary mirrors: I. Theory and elasticity design, *Astron. Astrophys. Suppl. Ser.*, **114**, 373-378
- Lubliner J. & Nelson J.E., 1980, KECK TELESCOPE: Stressed mirror polishing, *Appl. Optics*, **19**, 2332-2340
- Moretto G., Lemaître G.R., Bactivelane T., Wang W., Ferrari M., Mazzanti & Borra E.F., 1995, Active mirrors warped using Zernike polynomials for correcting off-axis aberrations of fixed primary mirrors: II. Optical testing and performance evaluation, *Astron. Astrophys. Suppl. Ser.*, **114**, 379-386
- Morse J.A., Green J.C., Ebbets D. & al., 1998, Performance and science goals of the Cosmic Origins Spectrograph / HST, in *Space Telescope and Instrumentation V*, Kona, HI, Proc. SPIE **3356**, 365-368
- Osterman S., Wilkinson E., Green J.C., and Redman K., 2000, FUV grating performance for the Cosmic origins spectrograph, in *UV, Optical and IR Space Telescope and Instruments*, Munich, Proc. SPIE **4013** 360-366
- Saint-Venant (Barré de) A., 1881, in *Résumé des Leçons de Navier sur l'Application à la Mécanique*, Dunod edit., Paris
- Schmidt B., 1932, *Mitt. Hamburg Strenv.*, **7**, 15
- Schmidt E., 1995, in *Optical Illusions - The life story of Bernhard Schmidt*, Estonian Academy Publ., ISBN 9985-50-102-0
- Su Ding-qiang, Cui Xiangqun, Wang Ya-nan, Yoa Zhengqiu, 1998, LAMOST, in *Advanced Technology Optical and IR Telescopes*, Proc. SPIE **3352**, 76-90
- Timoshenko S.P. & Woinowsky-Krieger S., 1959, in *Theory of Plates and Shells*, McGraw-Hill edit., 282
- Wang Min, 1992, Instrumentation astrophysique et optique active: Evaluation de TÉMOS-4, Doctoral thesis, Observatoire de Marseille, Université de Provence Aix-Marseille I
- Wang Shou-guan, Su Ding-qiang, Chu Yao-quan, Cui Xiangqun, Wang Ya-nan, 1996, LAMOST: Special configuration of a very large Schmidt telescope for extensive astronomical spectroscopic observation, *Appl. Opt.*, **35**, 25, 5155-5161
- Wilson R.N., 1999, in *Reflecting Telescope Optics II*, Springer edit. Berlin, chap.3
- Wilson R.N., Franza F., Noethe L., 1987, NTT - Active optics I, *J. of Modern Optics*, **34**(4), 485-511